

# Beyond pure parasystole: promises and problems in modeling complex arrhythmias

MARC COURTEMANCHE, LEON GLASS,  
MICHAEL D. ROSENGARTEN, AND ARY L. GOLDBERGER

*Department of Physiology, McGill University, Montreal, Quebec H3G 1Y6; Division of Cardiology, Montreal General Hospital, Montreal, Quebec H3G 1A4, Canada; and Cardiovascular Division, Beth Israel Hospital and Harvard Medical School, Boston, Massachusetts 02215*

COURTEMANCHE, MARC, LEON GLASS, MICHAEL D. ROSENGARTEN, AND ARY L. GOLDBERGER. *Beyond pure parasystole: promises and problems in modeling complex arrhythmias*. Am. J. Physiol. 257 (Heart Circ. Physiol. 26): H693–H706, 1989.—The dynamics of pure parasystole, a cardiac arrhythmia in which two competing pacemakers fire independently, have recently been fully characterized. This model is now extended in an attempt to account for the more complex dynamics occurring with modulated parasystole, in which there exists nonlinear interaction between the sinus node and the ectopic ventricular focus. Theoretical analysis of modulated parasystole reveals three types of dynamics: entrainment, quasiperiodicity, and chaos. Rhythms associated with quasiperiodicity obey a set of rules derived from pure parasystole. This model is applied to the interpretation of continuous electrocardiographic data sets from three patients with complicated patterns of ventricular ectopic activity. We describe several new statistical properties of these records, related to the number of intervening sinus beats between ectopic events, that are essential in characterizing the dynamics and testing mathematical models. Detailed comparison between data and theory in these cases show substantial areas of agreement as well as potentially important discrepancies. These findings have implications for understanding the dynamics of the heartbeat in normal and pathological conditions.

nonlinear dynamics; premature ventricular contractions; electrotonic interaction

---

VENTRICULAR PREMATURE CONTRACTIONS (VPCs) are a ubiquitous form of cardiac arrhythmia that can occur in otherwise healthy subjects or as a prelude to sudden cardiac death. Three major physiological mechanisms have been invoked to explain the genesis of these extra heartbeats (21): reentry, triggered activity, and parasystole (abnormal automaticity).

Reentry involves the presence of a “circular” conduction pathway in the myocardium. When specific conditions are met by the ventricular cardiac tissue, a depolarizing impulse can travel around the path and reexcite the heart after a fixed delay. This “circus movement” is reflected on the electrocardiogram (ECG) by VPCs that follow normal beats at a constant or nearly constant interval (fixed coupling). This type of fixed coupling pattern on the surface ECG can also arise with triggered activity. As the name implies, triggered VPCs result from depolarizations of sufficient amplitude induced by the

previous action potential. Finally, premature contractions can be elicited by an automatic focus located in the ventricles. The abnormal pacemaker periodically generates ectopic impulses that can cause VPCs. This mechanism is referred to as ventricular parasystole.

The basic mechanism for parasystole was proposed over 70 years ago (6), but the full range of rhythms it may produce has only recently been elucidated for the case when the two competing pacemakers fire independently of each other (7). In this situation, known as pure parasystole, the rhythms produced are very characteristic, and the dynamics of the arrhythmia are well understood.

If interaction between the pacemakers is allowed, the dynamics can become more complex. Schamroth and Marriott (30) postulated that the normal sinus rhythm could influence the firing pattern of a parasystolic pacemaker. Jalife and Moe (16) demonstrated in vitro that periodic electrotonic depolarizations of an active pacemaker protected from direct excitation can give rise to changes in its firing frequency. They developed a mathematical model that incorporates this property (23); depolarizations of sinus origin can affect the timing of ectopic pacemaker discharges. They called the resulting rhythms “modulated parasystole” and showed that the model can produce a rich variety of arrhythmic patterns, including some associated with fixed coupling intervals that simulate reentry or triggered activity (15, 23). They were also able to reproduce rhythms that are well known clinically, such as ventricular bigeminy and ventricular trigeminy, in which every second or third contraction of the heart is a VPC. Several groups of investigators subsequently identified modulated parasystole in clinical ECG recordings (4, 25, 27–29, 35). They determined the phase response curve, which gives the effect of a sinus depolarization on the period of the ectopic pacemaker as a function of its location within the ectopic cycle (see APPENDIX).

Theoretical aspects of modulated parasystole have also been studied by a number of workers (9, 14, 23, 31, 34). Mathematically, the problem of modulated parasystole can be cast in terms of the periodic stimulation and phase resetting of a cardiac oscillator (9, 14, 31). Although earlier studies showed that there are changes in the dynamics of modulated parasystole as a function of heart rate, several important features of modulated

parasyctole, and in particular its connection with pure parasyctole, have not been described previously. To appropriately treat the dynamics of modulated parasyctole, it is essential to adapt methods developed in a branch of mathematics called nonlinear dynamics. Such techniques have been highly successful previously in describing complex dynamics from periodically stimulated cardiac preparations (9, 10, 12, 13).

We carry out a detailed analysis of models for pure and modulated parasyctole and develop new tools to study clinical data from patients with frequent VPCs. In particular, we consider the values for the number of intervening normal beats (NIB) between successive VPCs. The distribution of NIB values for the whole record, the order in which they occur (transition matrix), and the variations in NIB values allowed as a function of heart rate are critical features that need to be accounted for by any model of ventricular ectopy. A complete theory of ventricular ectopy should be able to predict these statistical features as well as the changes in coupling intervals, given the variations in heart rate that actually occur in any patient.

In light of the results from the theoretical analysis and using the statistical tools described above, we study clinical data from three patients who demonstrate striking changes in the dynamics with variations in heart rate. These changes in heart rate occur as a result of three mechanisms: periodic stimulation of the human heart using an intra-atrial electrode, spontaneous periodic oscillations of heart rate in a patient prior to cardiac arrest, and normal beat-to-beat variability observed during daily activities.

**Glossary**

- $t_E$  Period of a ventricular ectopic pacemaker
- $t_S$  Period of the normal sinus pacemaker
- $\theta$  Refractory period of the heart. Measures length of time after initiation of a ventricular contraction during which the heart cannot be excited
- $\phi$  Phase of sinus beat in ectopic cycle. Time interval elapsed from depolarization of ectopic pacemaker divided by  $t_E$
- $T$  Modulated ectopic period due to a sinus beat at phase  $\phi$
- PRC Phase response curve. Gives dependence of  $T/t_E$  as a function of  $\phi$
- R On ECG, labels normal ventricular complex
- X On ECG, labels VPCs
- F On ECG, labels fusion beats with morphology intermediate to normal and ectopic beats

**THEORY**

*Pure parasyctole.* The theory and results for pure parasyctole have been discussed extensively in a previous publication (8). Briefly, the rhythm is determined by two parameters: the ratio of ectopic to sinus pacemaker periods ( $t_E/t_S$ ) and the length of the refractory period ( $\theta$ ), normalized to the sinus period ( $\theta/t_S$ ). The refractory period is defined as the length of time after a heartbeat during which the cardiac tissue is not susceptible to

further excitation. An ectopic discharge that falls during the refractory period does not produce a contraction and is termed a concealed ectopic beat. After each ectopic beat, we assume that the following scheduled sinus beat is blocked, resulting in a compensatory pause in cardiac activity. The model is illustrated schematically in Fig. 1A.

Figure 1B depicts the changes in the probability of observing a given NIB value as a function of  $t_E/t_S$  in the model for pure parasyctole, with  $\theta/t_S = 0.6$ . A summary of the results is found in Fig. 1C, which shows the allowed NIB values as a function of the two parameters ( $t_E/t_S$ ,  $\theta/t_S$ ). A set of four rules was derived with respect to these values: 1) for any ratio of  $t_E/t_S$  there are at most three different values of NIB; 2) one and only one of these

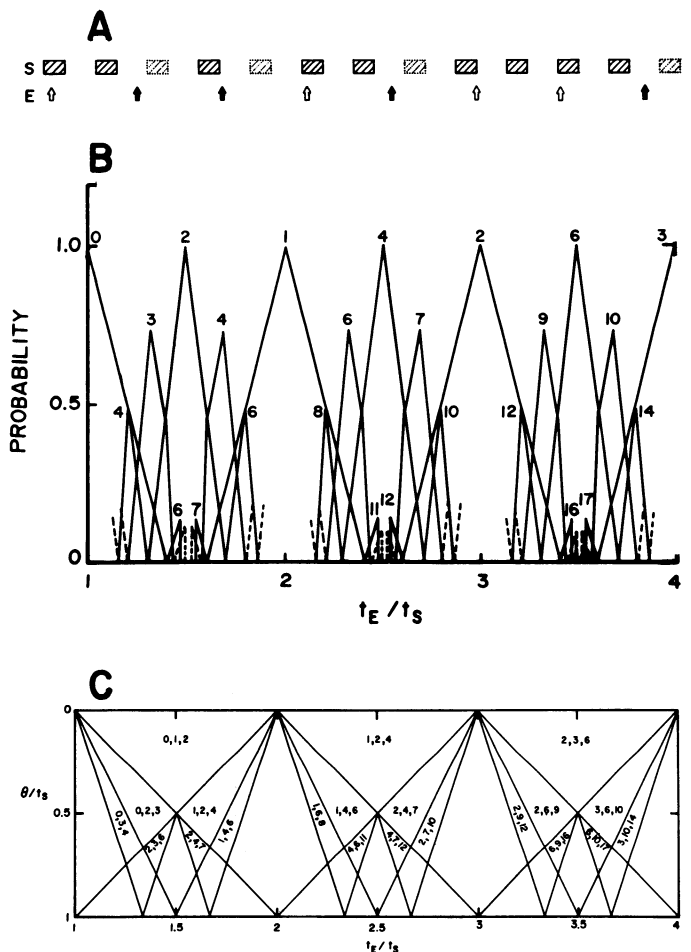


FIG. 1. A: schematic representation of model for pure parasyctole. Sinus rhythm (S) and ectopic rhythm (E) are shown. Refractory time is represented as a shaded region. Any ectopic discharge that falls outside refractory period gives rise to an ectopic beat (solid arrows). Subsequent sinus beat is blocked (dashed lines). Ectopic discharges falling during the refractory period are concealed (open arrows). In this simulation,  $t_E/t_S = 1.65$ ,  $\theta/t_S = 0.4$ . B: histogram showing the probability of observing a given NIB value as a function of  $t_E/t_S$ , with  $\theta/t_S = 0.6$ . For each value of  $t_E/t_S$ , the probability for each possible NIB is indicated. In the neighborhood of integers and half-integers, there is an infinite cascade of peaks that is too fine to be clearly represented by this graph. We give dotted lines to indicate this. C: allowed values for number of sinus beats between ectopic events (NIB) in the ( $\theta/t_S$ ,  $t_E/t_S$ ) plane for pure parasyctole. Allowed values in unlabeled regions can be determined using construction described in (8). See Glossary and text for definitions of other abbreviations.

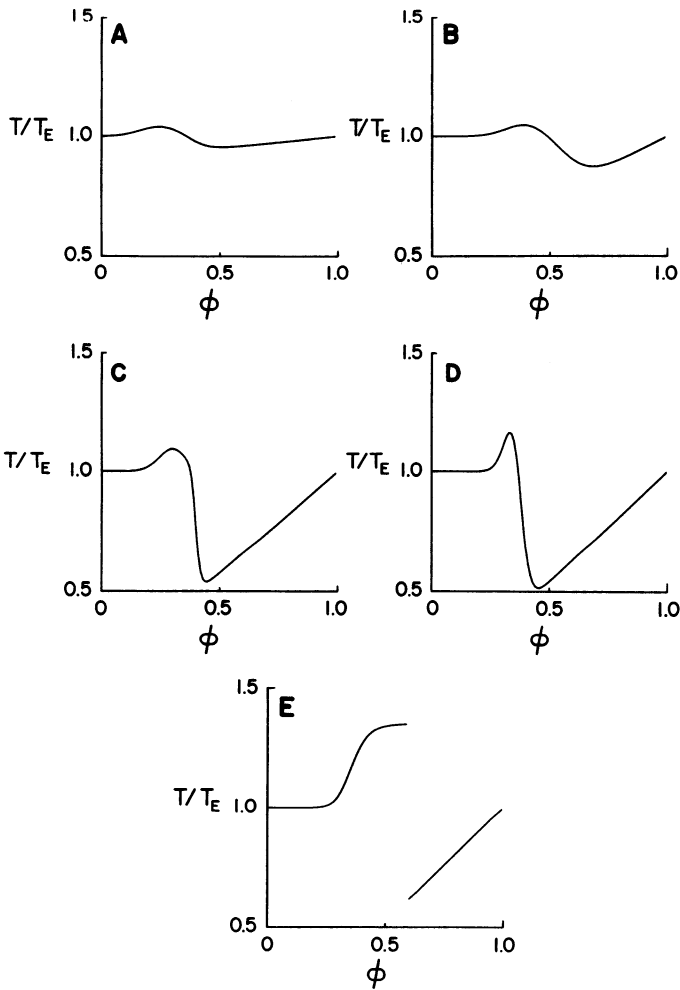


FIG. 2. PRC giving effect of a sinus beat on the ectopic cycle length as a function of its phase  $\phi$  within the cycle. Effect of modulation is given as ratio of perturbed cycle length divided by original cycle length  $t_E$ . Curves are ordered, from A to E, to generally reflect increasing coupling between pacemakers. Function used to plot curves A–D is described in Ref. 10.  $T/t_E(\phi)$  is given by  $1 + e^{-(\phi - \phi_{max})^2/\sigma^2} + S(\phi - 1)\phi^N/(\phi^N + \theta^N)$ . The parameters are A:  $C = 0.04$ ,  $\phi_{max} = 0.25$ ,  $\sigma = 0.12$ ,  $S = 0.1$ ,  $\theta = 0.4$ ,  $N = 10$ ; B:  $C = 0.05$ ,  $\phi_{max} = 0.4$ ,  $\sigma = 0.12$ ,  $S = 0.5$ ,  $\theta = 0.6$ ,  $N = 10$ ; C:  $C = 0.1$ ,  $\phi_{max} = 0.3$ ,  $\sigma = 0.08$ ,  $S = 0.85$ ,  $\theta = 0.4$ ,  $N = 40$ ; D:  $C = 0.215$ ,  $\phi_{max} = 0.35$ ,  $\sigma = 0.057$ ,  $S = 0.92$ ,  $\theta = 0.38$ ,  $N = 22.74$ . Curve E is derived from an analysis by Jalife et al. (15). For curve E,  $T/t_E(\phi)$  is given by  $1 + A\phi^{N_1}/(\phi^{N_1} + \theta^{N_1})$  if  $\phi < 0.6$  and  $1 + S(\phi - 1)\phi^{N_2}/(\phi^{N_2} + \theta^{N_2})$  if  $\phi \geq 0.6$ , where  $A = 0.35$ ,  $N_1 = 10$ ,  $\theta_1 = 0.36$ ,  $N_2 = 40$ ,  $\theta_2 = 0.6$ . See Glossary for definitions of other abbreviations.

three different values is odd; 3) if there are three possible values of NIB, the sum of the two smaller values is one less than the larger value; and 4) in any sequence of NIB in which three values are possible, only one of these can succeed itself.

**Modulated parasystole.** In modulated parasystole, sinus beats affect the period of the ectopic pacemaker. The phase  $\phi$  of a sinus beat in the ectopic cycle is defined as the time from the last ectopic discharge to the sinus beat divided by the ectopic pacemaker period  $t_E$ . A single sinus beat occurring at a phase  $\phi$  in the ectopic cycle results in a modulated ectopic period,  $T$ . The plot of  $T/t_E$  vs.  $\phi$  is called the PRC. Figure 2 gives five examples of PRCs that will be used in following simulations. The curves are ordered so that the level of coupling between

the pacemakers generally increases from Fig. 2A to Fig. 2E. Sinus beats at early phases either have little effect or cause a lengthening of the ectopic cycle; sinus beats at later phases trigger an ectopic discharge, i.e., cause a shortening of the cycle. The curves in this figure are typical of results found in model experimental systems (2, 10, 16) and clinical studies (15, 25, 27–29, 35).

Based on the PRC, it is possible to determine the effects of periodic perturbation of the ectopic focus by the sinus rhythm (9, 14, 23, 31). Calling  $\phi_i$  the phase of the sinus beat within the ectopic cycle, the phase  $\phi_{i+1}$  of the next sinus beat is given by

$$\phi_{i+1} = \phi_i + t_S/t_E \pmod{1}, \tag{1A}$$

$$0 \leq \phi_i < t_S/t_E - \theta/t_E,$$

$$\phi_{i+1} = \phi_i + 1 - T/t_E(\phi_i) + t_S/t_E \pmod{1}, \tag{1B}$$

$$t_S/t_E - \theta/t_E \leq \phi_i < 1$$

Given the phase of a sinus beat we can determine the context in which it occurred. If  $\phi_i \in [0, t_S/t_E - \theta/t_E]$ , the sinus beat is preceded by an ectopic beat and is blocked. This is the condition in Eq. 1A, and the blocked sinus beat does not modify the ectopic period. The next phase is obtained by adding the normalized sinus period  $t_S/t_E$ . If  $\phi_i \in [t_S/t_E - \theta/t_E, t_S/t_E]$ , the sinus beat is preceded by a concealed ectopic discharge and phase resets the ectopic pacemaker. The shift in phase resulting from the modulation of the ectopic period is given by the nonlinear term  $1 - T/t_E(\phi_i)$ , and the next phase is obtained using Eq. 1B. A sinus beat with phase  $\phi_i \in [t_S/t_E, 1]$  will also obey Eq. 1B and is preceded by another sinus discharge.

Figure 3 shows a plot of Eq. 1 obtained using the PRC

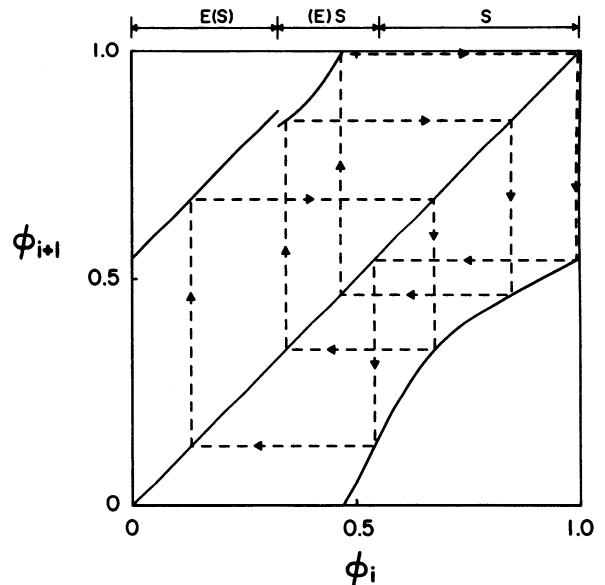


FIG. 3. Plot of Eq. 1 obtained using PRC of Fig. 2B. Function gives phase of next sinus beat,  $\phi_{i+1}$ , as a function of the previous phase  $\phi_i$ . Identity line, along which  $\phi_{i+1} = \phi_i$ , is also plotted. The 3 regions above graph represent different contexts for a sinus beat depending on value of its phase. E(S), blocked sinus beat preceded by ectopic beat; (E) S, sinus beat preceded by a concealed ectopic beat; S, single sinus beat. Dashed lines represent graphical iterations of function. Cycle containing 7 phases arises for this simulation in which  $t_S/t_E = 0.544$  and  $\theta/t_S = 0.4$ . See Glossary for definitions of other abbreviations.

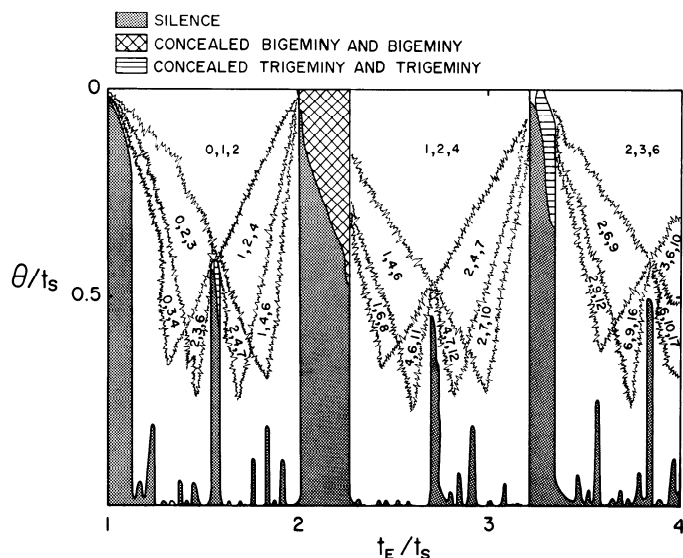


FIG. 4. Allowed NIB values for modulated parasystole in the  $(\theta/t_s, t_E/t_s)$  plane, using the PRC of Fig. 2B. Where triplets of NIB values are indicated, any combination of the 3 values may be present. Jagged boundaries reflect extremely irregular nature of borders separating different zones. Dotted regions are devoid of ectopic activity (silence) and usually associated with entrainment zones. Regions of bigeminy and trigeminy are indicated. See *Glossary* and text for definition of abbreviations.

of Fig. 2B, with  $t_s/t_E = 0.544$  and  $\theta/t_s = 0.4$ . The three intervals discussed above are identified along the top abscissa. The equation can be iterated graphically, as shown by the dashed lines. Each intersection of the dashed lines with the curve represents a value of  $\phi_i$  in the iteration. The function displays a noticeable jump at  $\phi_i = t_s/t_E - \theta/t_E$ , i.e., it is discontinuous at that point. The other break in the curve, when  $\phi_{i+1} = 1$ , results from taking all phases *modulo* 1. In this example, the cycle contains seven different phases. Phases in  $[0, t_s/t_E - \theta/t_E]$  are assigned to blocked sinus beats preceded by an ectopic beat. By counting the number of iterations required to return into this interval, we get the values for NIB. In this case a single NIB value is allowed, NIB = 6.

In general, analysis of nonlinear equations such as Eq. 1 reveals three distinctly different types of dynamics. These are phase locking (entrainment), quasiperiodicity, and chaotic dynamics. We discuss each separately and give a pertinent example.

Entrainment is characterized by a periodic pattern of sinus and ectopic discharges. We refer to  $N:M$  entrainment when there are  $N$  sinus discharges, for every  $M$  ectopic impulses. All sinus and ectopic beats are included, even those that are blocked. As an example, consider the entrainment pattern associated with ventricular bigeminy. In this rhythm there are two sinus beats, one of which is blocked, for each ectopic discharge (2:1 entrainment). Another example can be found in Fig. 3, which shows 7:4 entrainment. Of the four ectopic discharges present in the cycle, three are concealed, resulting in a single NIB value.

Figure 4 shows the allowed NIB values in different regions of the  $(\theta/t_s, t_E/t_s)$  parameter space for modulated parasystole. We again use the PRC of Fig. 2B. Figure 4

also depicts zones where ectopic activity is abolished (silence) and regions of bigeminy and trigeminy. Within each zone where triplets of values are possible, there may sometimes be only one or two of these present. The structure within each of these regions, and especially at the boundary, can be extremely complex. The jagged boundary lines are meant to schematically represent the borders between the different regions. Usually, major entrainment zones are associated with an area of silence. For example, the large silent area between  $t_E/t_s \approx 2$  and  $t_E/t_s \approx 2.25$  corresponds to 2:1 entrainment. The possible rhythms within the major entrainment zones depend on the value of the repeating phases generated by Eq. 1.

Rhythms associated with bigeminy arise near the 2:1 entrainment zone. As  $t_s$  increases, at first only a single value of NIB, NIB = 1, corresponding to bigeminy is allowed. Then, the rhythms undergo a sequence of qualitative changes, called bifurcations, giving rise to  $N:M$  entrainment ratios where  $N/M = 2$ . This corresponds to values of NIB that are of the form  $2n - 1$ , where  $n$  is an integer. Such rhythms, in which only odd NIB values occur, are called concealed bigeminy (28). These bifurcations are associated with the discontinuity of the phase resetting function at  $\phi_i = t_s/t_E - \theta/t_E$ . As  $t_s$  increases further the dynamics fall back into 2:1 entrainment but within the silent area. Similar changes can be seen in the 3:1 zone. In this case, as  $t_s$  increases, the NIB values go from 2 (trigeminy) to  $3n - 1$  (concealed trigeminy) to silence. Trigeminy and concealed trigeminy also occur within the 3:2 entrainment zone. The regions of concealed rhythms occupy a relatively narrow range of parameter values compared with bigeminy or silence. As the interaction between the pacemakers becomes stronger or the refractory period increases, the expressed ectopic rhythms become "squeezed out" and only silence is observed.

Quasiperiodicity can be defined as aperiodic dynamics for which two initial phases close enough together remain close under iteration of Eq. 1, and each phase eventually gets arbitrarily close to any value in the interval  $[0, 1]$ . Given certain conditions on Eq. 1, including quasiperiodicity, we can show that the rules for pure parasystole apply to modulated parasystole (unpublished results). In many cases, Eq. 1 is discontinuous, and the dynamics are not quasiperiodic. Despite this, the behavior of the system is apparently very close to quasiperiodicity for some parameter values when the effect of the discontinuity is small. An example of this is presented in Fig. 5 in the form of a simulated simplified ECG, with allowed NIB values of 1, 6, and 8 consistent with the rules of pure parasystole. The simulation uses the PRC of Fig. 2D, characteristic of strong coupling between the pacemakers, with  $\theta/t_s$  set at 0.3.

In general, weak interaction between the pacemakers, as shown in Fig. 4, gives rise to small entrainment zones and mostly rhythms that obey the new rules of pure parasystole reported in Ref. 8. The similarities between Fig. 1C and Fig. 4 reflect this fact. The rules for pure parasystole can also be observed when stronger interaction occurs between the pacemakers, as in Fig. 5.

Chaotic dynamics can also be found in Eq. 1. Chaos refers to aperiodic dynamics that are extremely sensitive

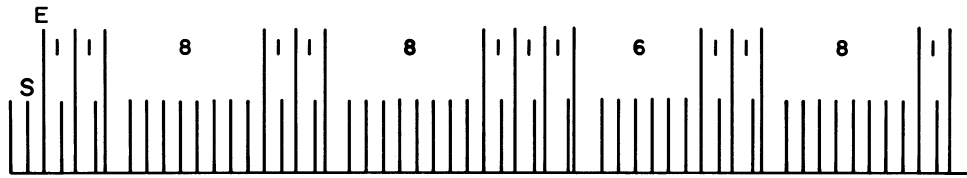


FIG. 5. Simulated simplified ECG illustrating dynamics of modulated parasystole that obey the rules for pure parasystole, using PRC of Fig. 2D. Short bars (S) correspond to normal sinus beats. Long bars (E) represent ectopic beats. NIB values are indicated above. Parameters are  $t_s/t_E = 0.514$ ,  $\theta/t_s = 0.3$ . See *Glossary* and text for definition of abbreviations.

to initial conditions and is the subject of intense research in the field of nonlinear dynamics. One definition of chaos is a positive Liapunov number.<sup>1</sup> The Liapunov number measures the sensitivity of the dynamics to initial conditions by estimating the rate of divergence of nearby phases during the iteration process (37).

Chaos is found in Eq. 1 using the PRC of Fig. 2D with  $t_E/t_S = 2.15$  and  $\theta/t_S = 0.4$ . The sharpness of the transition between the lengthening and shortening effect of sinus beats in the PRC of Fig. 2D produces a region of large positive slope in Eq. 1. This seems to provide the expansion property necessary to generate chaotic dynamics. Figure 6A shows 500 graphical iterations, obtained after discarding the first 1,000 iterations. The values of the phase are plotted as pairs  $(\phi_i, \phi_{i+1})$ . Successive values cover most of the curve and give an outline of the shape of Eq. 1. We computed an estimate for a positive Liapunov exponent of 0.087. The allowed values for NIB are 3, 6, 9, 10, and 13, and a simulated sequence is shown in Fig. 6B. This is the first demonstration of chaotic dynamics in a mathematical model of parasystole. However, it is not yet clear how to systematically identify PRCs that can produce chaotic dynamics.

CASE REPORTS

The dynamics of parasystole depend on a number of parameters, including heart rate, ectopic pacemaker rate, excitability of cardiac tissue, conduction properties, and the degree of interaction between the pacemakers. In any subject, many or all of these parameters undergo beat-to-beat changes that may affect the rhythms observed. The richness and complexity of long rhythm strips may depend on these variations, and any attempt to completely understand any clinical record must include a detailed analysis of the data. This is in contrast to the common clinical practice of summarizing long and complex electrocardiographic records with a few gross characteristics such as frequency of VPCs within given time periods. The following reports are intended to support our contention that detailed analysis can provide insight into the mechanism of arrhythmias and to show the

extent to which models for parasystole can explain the clinical data.

In the analysis of the first and third case reports, clinical tracings were digitized using a Hewlett-Packard Graphics Tablet linked to a HP 9816 computer. All the intervals between successive ventricular activations were digitized to an accuracy of  $\pm 20$  ms. Analysis of the second case was carried out directly from the data (digitized onto magnetic tape) using a beat recognition algorithm (24)

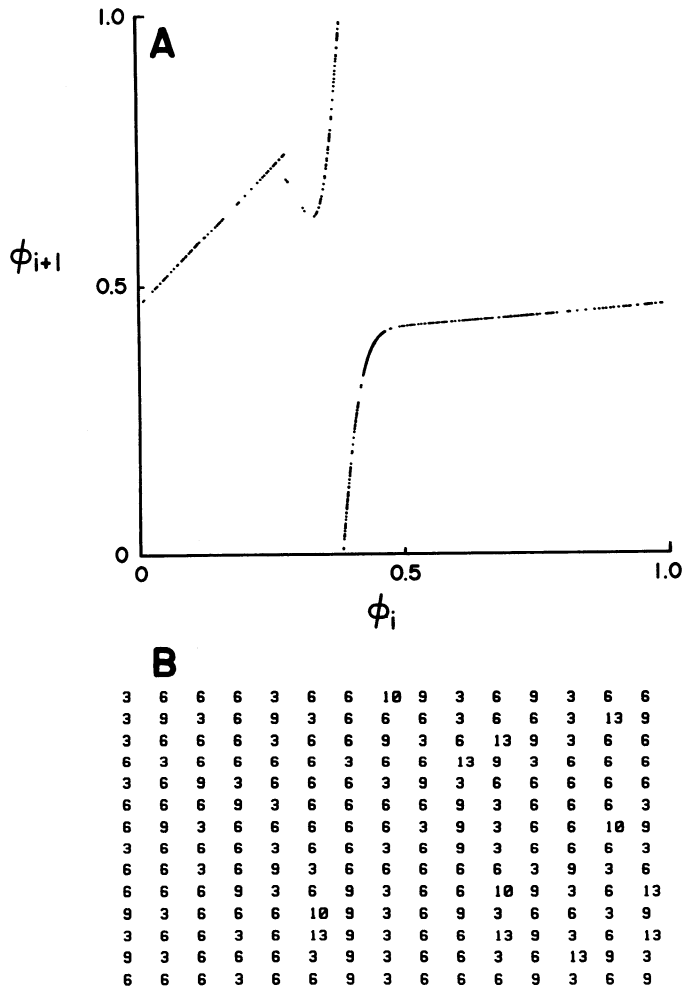


FIG. 6. A: chaotic iterates of Eq. 1 obtained using PRC in Fig. 2D, with  $t_s/t_E = 0.465$  and  $\theta/t_S = 0.4$ . Each point  $(\phi_i, \phi_{i+1})$  is an iterate of Eq. 1 placed on curve at its appropriate location. There are 500 iterates that were plotted after discarding 1,000 iterations. We computed a positive Liapunov exponent, 0.087, indicating chaotic dynamics (37). B: NIB sequence resulting from simulation in A. NIB values allowed are 3, 6, 9, 10, and 13. See *Glossary* and text for definition of abbreviations.

<sup>1</sup>The Liapunov exponent for one-dimensional finite-difference equations such as Eq. 1 is defined by

$$L = \lim_{n \rightarrow \infty} - \sum_{i=1}^n \log |df/d\phi_i|$$

where  $df/d\phi_i$  is the first derivative of Eq. 1 and evaluated at successive iterates  $i$  of Eq. 1 (32). In the text we computed an estimate of  $L$  by taking  $n = 20,000$ , after discarding the first 1,000 iterations to minimize any transient behavior.

that extracted information about the relevant intervals. Informed consent was obtained from the three patients in this report.

*Case 1: periodic stimulation of a human heart.* We present the results of a periodic stimulation study on a middle-aged man with frequent ectopy and syncope, obtained as part of an electrophysiological study. We first recorded 5 min of ECG at resting heart rate. Then, using intracardiac pacing, the patient underwent pacing runs of 1 min, with stimulation periods varying from 600 down to 400 ms in steps of 50 ms.

Figure 7 summarizes our results. Figure 7, strips A–E are excerpts from the study for each stimulation period. At the end of each strip is a histogram showing the distribution of NIB values for that stimulation period (Fig. 7, open bars). The resting heart period is close to 600 ms, so that the base-line rhythm is similar to Fig.

7A. In all strips, interectopic intervals are roughly multiples of a common divisor,  $\sim 1,050$  ms, within the range of precision of our measurements. Fusion beats of intermediate morphology between normal (R) and premature beats (X), as well as variable coupling intervals, are observed in Fig. 7, strips A, B, D, and E. These findings are consistent with the classical criteria used by cardiologists to identify pure parasystole on the ECG (17), and a careful examination of the NIB values found in these four strips show good agreement with the new rules described above for pure parasystole. The three values most often observed in these strips follow the rules exactly except for the observation of an NIB value of 9 (rather than 7) in Fig. 7, strip E. Examination of Fig. 7, strip C however, reveals a concealed bigeminal rhythm, at a stimulation period where  $t_E/t_S$  is close to 2. In Fig. 7, strip C, coupling intervals are fairly constant. This

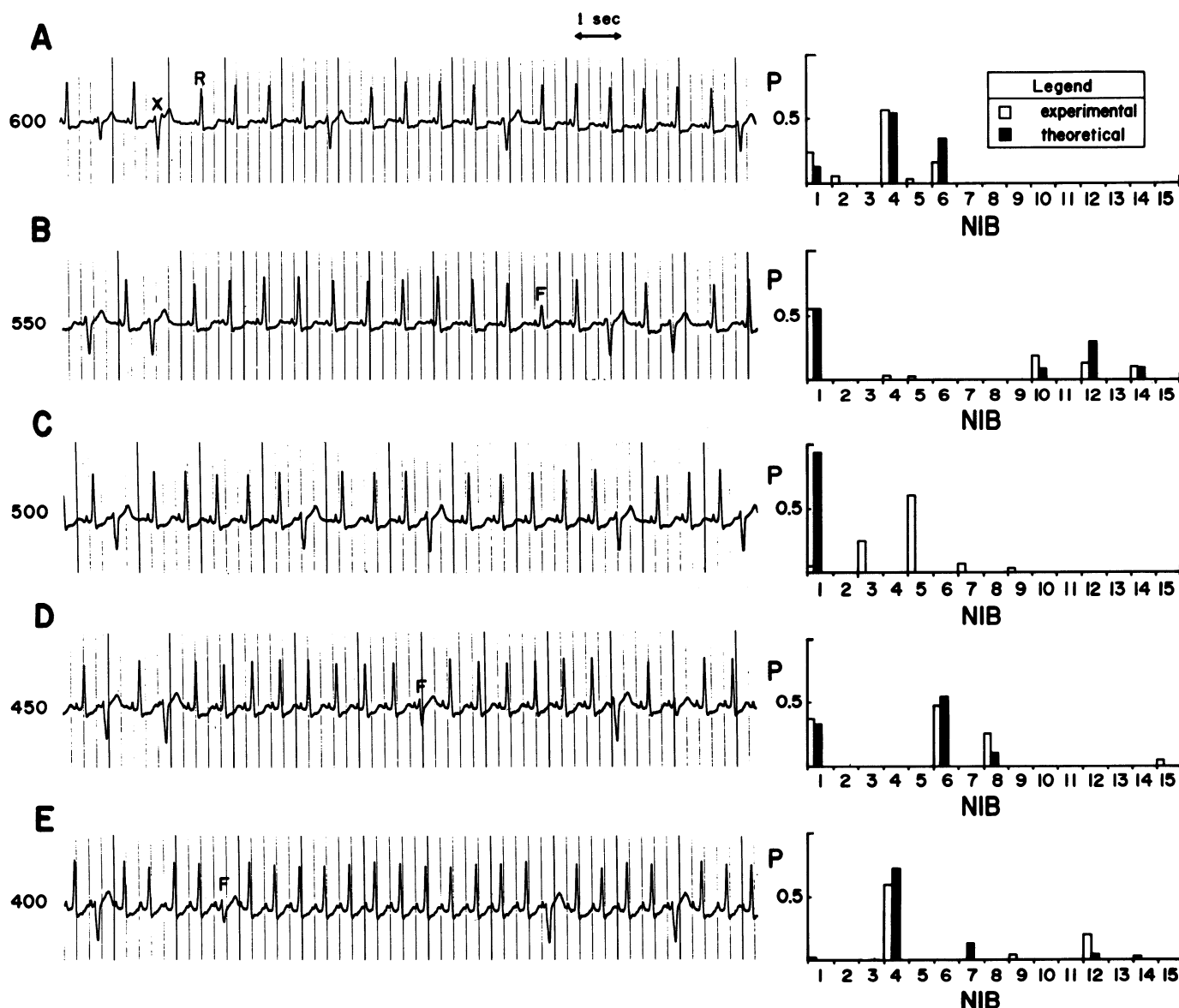


FIG. 7. Results from periodic stimulation study. A–E are excerpts from study. Pacing periods ( $t_S$  in ms) are indicated on left of each strip. A VPC (X) and a normal beat (R) are indicated in A. Fusion beat (F) is labeled in B. On right of each strip, a histogram gives probabilities ( $P$ ) of NIB values observed during pacing run (open bars). Predicted values (solid bars) from theoretical model are also indicated. See *Glossary* and text for definition of other abbreviations.

cannot be explained by pure parasystole but is consistent with modulated parasystole.

We postulate that weak interaction is taking place between the pacemakers that is not strong enough to produce measurable change in the ectopic pacemaker period but is sufficient to give rise to an entrainment pattern when the ratio of the two pacemaker frequencies is close to an integer. We assume a PRC that produces a maximum change of 4% in the ectopic pacemaker period (Fig. 2A). This is within the range of error in our measurements. The refractory period is determined by measuring the value of the smallest R-X interval at each frequency. All values of  $\theta/t_S$  are between 0.6 and 0.75.

Results of the simulation are shown in Fig. 8 as a histogram that gives the probability of observing a given NIB value as a function of  $t_E/t_S$ , with  $\theta/t_S = 0.6$ . Figure 8 is a good example of the complexity involved in analyzing the dynamics of modulated parasystole in great detail. The lines drawn in Fig. 8 represent a smoothed histogram, i.e., straight lines that follow the contour of histogram curves that are intrinsically jagged. The jaggedness is due to the numerous entrainment zones that cause the histogram to vary discontinuously, not unlike the borders of the zones in Fig. 4. Most peaks would show a break at their highest probability value, corresponding to an entrainment zone near a rational value of  $t_E/t_S$ .

Taking  $t_E = 1,050$  ms in our experiments, we can locate Fig. 7 strips A-E along the  $t_E/t_S$  axis. In cases Fig. 7, A, B, D, and E, the NIB values allowed by the model correspond to the major values in the histogram for each case, (solid bars in Fig. 7). For Fig. 7, strip C, the model predicts bigeminy instead of concealed bigeminy. Inspection of Fig. 8, however, reveals that a decrease of only 40 ms in the approximate value of  $t_E$  shifts the model into the zone of bifurcations associated with concealed bigeminal rhythm. Some additional values for NIB are observed in the experiment, which may be explained by

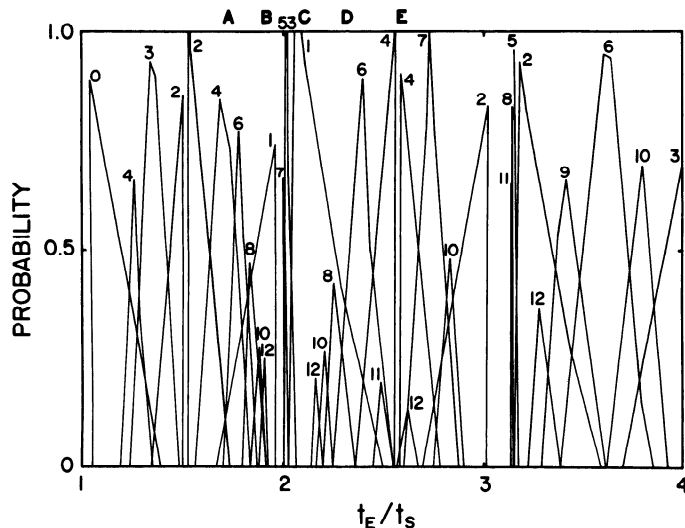


FIG. 8. Histogram showing probability of observing a given NIB value as a function of  $t_E/t_S$ . This simulation of pacing study uses the PRC of Fig. 2A.  $\theta/t_S$  is set at 0.6. Parameter values corresponding to A-E in Fig. 7, using  $t_E = 1,050$  ms, are shown along top abscissa. Only NIB values between 0 and 12 are included. See Glossary and text for definition of abbreviations.

changes in refractory time. For example, in Fig. 7, strip D, the predominant values are 1, 6, and 8, but 15 can also be found. Consider the sequence where a 6 is followed by an 8 in Fig. 7, strip D. The expression of the ectopic beat that separates the two interectopic intervals is dependent on the preceding refractory period. A slight prolongation could conceal the discharge, resulting in  $NIB = 6 + 8 + 1 = 15$ .

If only a weak level of modulation exists, we expect the data to obey the rules for pure parasystole in certain parameter regions. This is because, for weak modulation, the nonlinearity of Eq. 1 is small, and thus the form of Eq. 1 will be close to Eq. 1A for all phases. This is the equation used for pure parasystole. The transition matrix gives the probability that a given NIB value will occur as a function of the preceding value. Figure 9A gives the transition matrix for the NIB values in Fig. 7, strip A. Figure 9B shows the same transition matrix for a simulation in which  $t_E/t_S$  was picked to reproduce the NIB histogram for Fig. 7, strip A, using  $t_E/t_S = 1.75$  and  $\theta/t_S = 0.6$ . Because the probabilities for each NIB are identical in both cases, we obtain results that are not biased by different NIB distributions. In both cases 1) 4 is the only NIB that can succeed itself; 2) a 1 is almost always followed by a 4; and 3) a 6 can only be followed by a 4. All of these are consistent with the rules for pure parasystole and show these rules apply to quasiperiodic rhythms in modulated parasystole.

In summary, this case illustrates a striking degree of agreement between the theoretical model and the clinical case as stimulation parameters are varied.

*Case 2: periodic heart rate dynamics and ventricular bigeminy prior to cardiac arrest.* As our second case, we consider a patient in whom pathological heart rate fluctuations occur in a very orderly fashion. The patient has frequent VPCs in a ventricular bigeminal rhythm. Figure 10A shows a section of ECG from the subject recorded 3 h prior to cardiac arrest with ventricular fibrillation. We can count a single sinus beat (R) between the two ectopic beats (X). Figure 10C gives a heart rate plot based on the value of successive intervals between ventricular activations. The relatively smooth traces represent regions of normal rhythm, whereas the jagged sections are associated with episodes of ventricular bigeminy. This type of heart rate periodicity has been associated with Cheyne-Stokes breathing, a regular waxing and waning of ventilation most commonly seen with congestive heart failure or central nervous system dysfunction (6). A traditional clinical analysis would conclude at this point with a qualitative description of long bigeminy runs and periods of normal sinus rhythm. However, more detailed examination of the bigeminy runs reveals striking oscillations in the values of the X-R (ectopic-sinus) and R-X (sinus-ectopic) intervals, as shown in Fig. 10B. Although the phase relationship is not identifiable by visual inspection of Fig. 10C, the oscillations in X-R intervals are in phase with the R-R interval fluctuations, for which we measure a period of 43 s and an amplitude of 105 ms around a mean value of 900 ms.

If the observed rhythm is modulated parasystole, the response of the ectopic pacemaker to sinus depolarizations can be determined by studying the relation between

		NIB(i+1)					
A		1	2	3	4	5	6
NIB(i)	1	-	0.12	-	0.08	-	-
	2	0.50	-	-	-	-	0.50
	3	-	-	-	-	-	-
	4	0.37	-	-	0.34	0.02	0.24
	5	1.00	-	-	-	-	-
	6	-	-	-	1.00	-	-

		NIB(i+1)					
B		1	2	3	4	5	6
NIB(i)	1	-	-	-	1.00	-	-
	2	-	-	-	-	-	-
	3	-	-	-	-	-	-
	4	0.42	-	-	0.35	-	0.23
	5	-	-	-	-	-	-
	6	-	-	-	1.00	-	-

FIG. 9. Transition matrix giving probability that a given NIB value, NIB (i + 1), will occur as a function of the preceding value, NIB (i). A: calculated from first pacing run in experiment. B: computed from theoretical model (PRC of Fig. 2A,  $t_s/t_E = 0.57$ ,  $\theta/t_s = 0.6$ ). See Glossary and text for definition of abbreviations.

X-R and X-X intervals (see APPENDIX). The slope of the PRC for large phases is related to the change in R-X vs. X-R in Fig. 10B. A change of  $y$  ms in X-R yields a change of  $0.85y$  in the value of the X-X interval. This sets the slope of the last portion of the PRC to 0.85. The crossover between lengthening and shortening effects should be less than the smallest phase of a sinus beat in the bigeminal rhythm. An approximate value for the ectopic cycle length is determined so that bigeminy results within the range of sinus rates observed.

When the slope of the last portion of the PRC is as high as 0.85, there is close coupling of sinus beats to ectopic discharges, and the region of silence is prominent within the 2:1 entrainment zone where bigeminy arises. We need to assume a conduction time outside the ectopic pacemaker region to obtain a sustained bigeminal rhythm. Conduction time cannot be determined directly from the data but can be obtained given a value of  $t_E$  and the slope of the last portion of the PRC. We compute a conduction time of 380 ms with  $t_E$  set at 2.75 s and the PRC given in Fig. 2C.

Including sinusoidal variation of the heart rate with the period and amplitude indicated above, we obtain the theoretical fluctuations in interval lengths plotted in Fig. 11. The simulation agrees well with the data of Fig. 10B, although the X-R intervals are longer in the simulation.

In the model, the time between two sinus beats separated by an ectopic beat is twice the sinus period. This is not the case in the data. The intervening ectopic beat may be affecting the timing of the following sinus beat. The model also lacks the irregularity of the clinical data. This is probably associated with lower scale variations in sinus rate. The simulation does agree with the data both in terms of the relative amplitude of the interval oscillations and their mutual phase relationships.

Case 3: frequent ventricular ectopy during ambulatory monitoring. Long rhythm strips provide a great deal of information about the dynamics of the heart. However, their interpretation is a challenge due to the complex fluctuations in many parameters and the difficulty in establishing a definite mechanism. To illustrate these points, we consider a 30-min section from a 24-h ambulatory ECG recording in a patient with frequent ectopy. We apply the statistical tools introduced earlier to decode the detailed structure of the rhythm.

A section of ECG from the trace is displayed in Fig. 12. The NIB values observed in this section are 1, 4, 3,

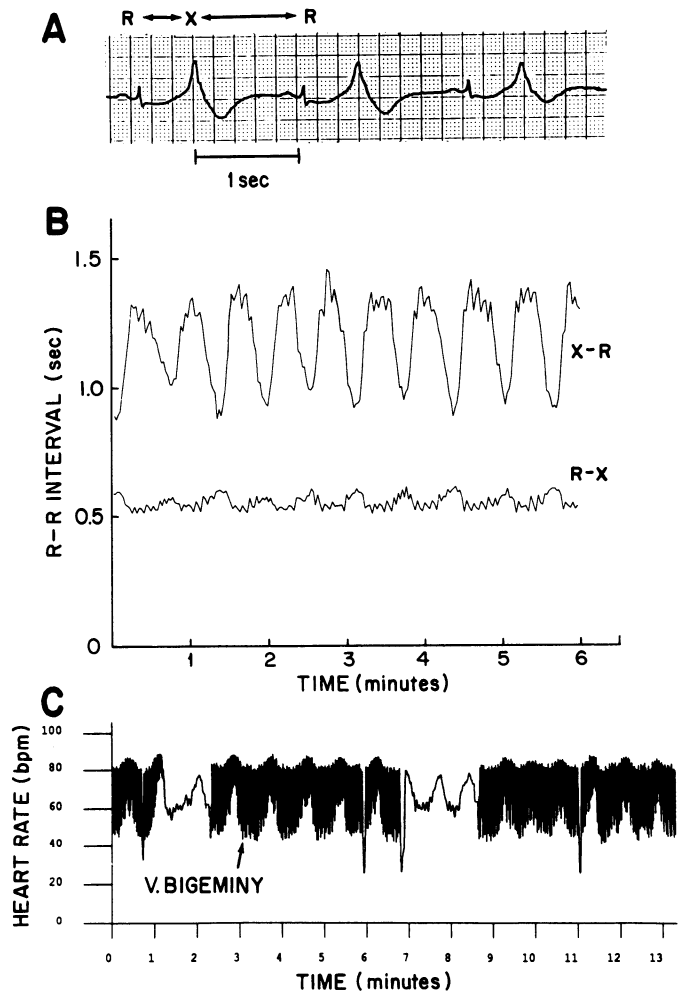


FIG. 10. A: rhythm strip from our patient during a bigeminal rhythm. Normal (R) and premature (X) beats are indicated. B: variations in X-R and R-X intervals during a section of bigeminal rhythm. The 2 oscillations are 180° out of phase. X-R oscillations are in phase with fluctuations in sinus R-R intervals (not shown). C: oscillations in heart rate occurring in same patient. Jagged trace is associated with ventricular bigeminy. See Glossary for definition of abbreviations.



NIB(i)	NIB(i+1)									total
	1	2	3	4	5	6	7	8	>8	
1	0.63	-	0.09	0.15	0.02	0.06	0.01	0.01	0.05	0.39
2	0.50	0.25	-	-	-	-	-	-	0.25	0.01
3	0.33	-	0.27	0.24	0.03	0.04	0.01	0.02	0.06	0.24
4	0.05	0.03	0.52	0.10	0.03	0.03	0.03	0.03	0.00	0.19
5	0.30	-	0.15	0.00	0.15	-	0.00	-	0.15	0.03
6	0.33	-	0.25	0.29	-	0.00	-	-	0.04	0.05
7	0.11	-	0.56	0.22	-	0.11	-	-	-	0.02
8	0.29	-	0.14	0.29	0.14	-	-	-	0.14	0.01
>8	0.27	-	0.20	0.20	0.03	0.10	0.10	0.03	0.07	0.06

FIG. 14. Transition matrix computed from NIB sequence of Fig. 13B. Last column indicates total probability of observing each NIB value. See *Glossary* and text for definitions of abbreviations.

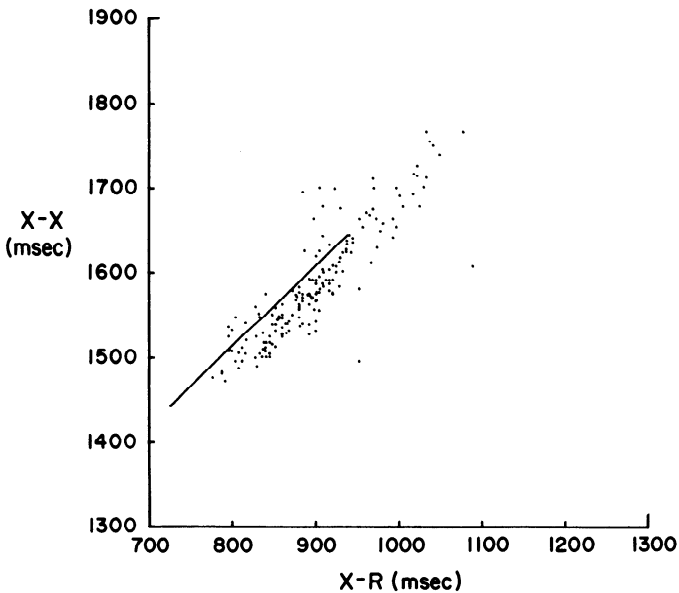


FIG. 15. Plot of X-X vs. X-R intervals measured from long rhythm strip, for the cases where NIB = 1. Slope is close to 1, reflecting relatively fixed R-X intervals in record. The 2 points corresponding to shorter X-X intervals are associated with an infrequent second morphology of VPCs. Solid line has a slope of 0.95 and shows range of X-R intervals spanned by simulation for interectopic intervals containing a single sinus beat (see text). See *Glossary* and text for definition of abbreviations.

of nearly 400 NIB values during the 30-min observation, only four values of 2 are observed. In preliminary simulations using various forms for the PRC, we found it very hard to reproduce the observed dynamics without also obtaining NIB values equal to 2. The most accurate predictions were obtained when we considered that the second sinus beat in an interectopic interval caused a delay of the next ectopic discharge beyond the third sinus beat. This is obtained with the PRC of Fig. 2E, which gives rise to a large delay of 35% in the ectopic cycle length for phases <0.6. A final assumption involves changes in the length of the refractory period induced by ectopic activity. Experiments by Lee et al. (18) on the hearts of dogs have shown that the length of the refractory period increases after a compensatory pause. As

cardiac activity resumes at the normal rate, the refractory period returns exponentially to its steady-state value. This feature is consistent with other studies that have shown that the refractory period after a cardiac excitation is dependent on the time since the previous contraction (17, 22, 33). These observations are included in the model by taking the refractory period to be 80% of the time since the last contraction. We also allow  $\pm 10\%$  random fluctuations in the refractory time.

Using the sequence of R-R intervals obtained from the patient, we can implement the model for modulated parasystole with the above features. Figures 16 and 17 present the results of the simulation using the same techniques as in Figs. 13 and 14. The model accurately predicts the major change in the dynamics observed in the record, displaying mainly NIB values of 1 early in the record and NIB values of 3 and 4 after the decrease in heart rate (Fig. 16A). Because the R-R intervals are taken directly from the patient and the R-X intervals in the model are fairly constant around 700 ms as in the

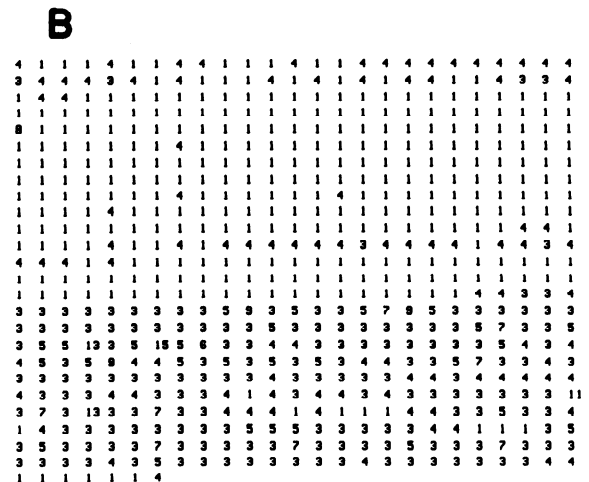
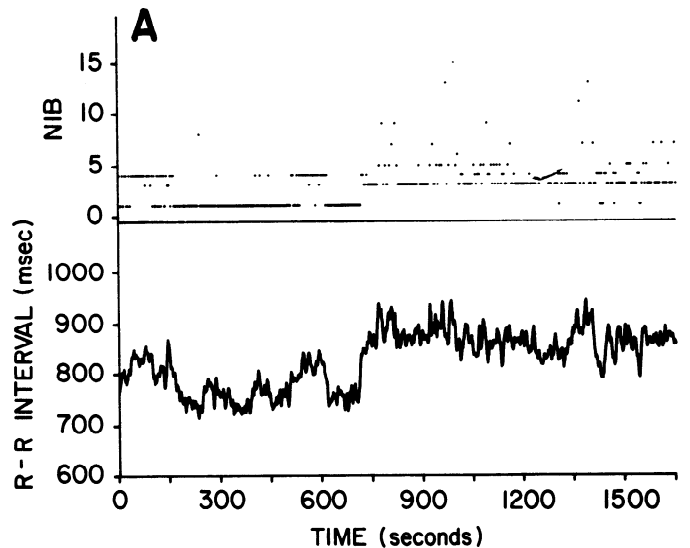


FIG. 16. A: plot of R-R intervals and NIB values vs. time obtained from model for modulated parasystole (see Fig. 13A). PRC used is shown in Fig. 2E. Anterograde and retrograde conduction are both equal to 350 ms. See text for details. B: sequence of NIB values resulting from simulation. See *Glossary* and text for definition of abbreviations.

		NIB(i+1)									
		1	2	3	4	5	6	7	8	9	total
NIB(i)	1	0.91	-	0.00	0.00	-	-	-	0.00	0.00	0.51
	2	-	-	-	-	-	-	-	-	-	-
	3	-	-	0.70	0.14	0.12	-	0.03	-	0.01	0.26
	4	0.29	-	0.23	0.46	0.02	-	-	-	-	0.15
	5	-	-	0.56	0.04	0.11	0.04	0.11	-	0.15	0.04
	6	-	-	1.00	-	-	-	-	-	-	0.00
	7	-	-	0.08	-	-	-	-	-	0.13	0.01
	8	1.00	-	-	-	-	-	-	-	-	0.00
	9	-	-	0.50	0.25	0.25	-	-	-	-	0.01

FIG. 17. Transition matrix computed from NIB sequence of simulation in Fig. 16B. Last column indicates total probability of observing each NIB value. See *Glossary* and text for definition of abbreviations.

patient, there is good correspondence between the intervals observed in the model and those seen in the patient. The solid line of Fig. 15 depicts the range of values for the pairs (X-R, X-X) obtained from the simulation when NIB = 1. One restriction of the model is that it allows very few values for NIB other than the major values at each heart rate level. This is in contrast to the clinical data, especially in the early section (800 s), which displays some large NIB values along with even and odd values >1. The transition matrix for the simulation (Fig. 17) reveals that the model works well in predicting the grouping of bigeminal sequences but fails to agree with the transition probability for NIB = 4. A value of 4 is frequently followed by a 1 in the simulation but very rarely in the clinical record. This important feature is not accounted for by the model, which also fails to produce NIB values equal to 2. Only a few of these are present in the data and in every case they are associated with fusion beats. These discrepancies clearly illustrate the unresolved problems that arise when trying to account for such complex rhythms using a simple model of modulated parasystole.

DISCUSSION

In previous work (8), we considered the dynamics of pure parasystole and attempted to understand the rhythms that arise in this situation. Studying this simple model gives some insight into the workings of parasystolic rhythms, from which we can approach the problem of modulated parasystole. Previous investigations of the dynamics of modulated parasystole have concentrated on the entrainment patterns between normal and ectopic pacemakers. By analyzing a model for modulated parasystole, we find that rhythms obeying theoretical rules for pure parasystole also exist outside the entrainment zones. We also give a theoretical example of chaotic dynamics arising in modulated parasystole and provide some insight into the bifurcations involved in the generation of concealed rhythms. The first clinical study shows the transition between “quasiperiodic” and entrained rhythms in a pacing experiment and introduces

statistical tools to be used in decoding the fine structure of clinical records. These techniques can highlight the complexity of long ECG records, as shown by the third case report. To our knowledge, this is the first attempt at reproducing such a long rhythm strip using a model for modulated parasystole and clearly illustrates the problems involved.

*Modulated parasystole in previous reports.* Because they can arise in the context of modulated parasystole, rhythms that obey the rules of pure parasystole, may not always display interectopic intervals that are multiples of a common divisor. Levy et al. (19) described a variant of concealed bigeminy in which runs of bigeminy (NIB = 1) are interrupted by even NIB values (2 cases). Within the bigeminy runs, the coupling interval between sinus and ectopic beats gradually decreases. Fusion beats are present, but pure parasystole is ruled out because interectopic intervals are not multiples of a common divisor. All these features can be found in the simulation of Fig. 5, which obeys the theoretical rules for pure parasystole where only one or an even number of sinus beats is allowed between ectopic beats. We can also observe similar rhythms in entrainment zones with complicated *N/M*.

Another example arises in a recent clinical study that considers the changes in the distribution of NIB values as a function of heart rate. Nilsson et al. (26) have examined the pattern of NIB values in 24-h ambulatory ECG recordings from patients with frequent VPCs. In one patient, they observed a transition from silence to concealed bigeminy followed by trigeminy as the heart rate increased. They postulate that the underlying mechanism may be modulated parasystole because the changes obey the sequence observed in the theoretical models. In fact, very strong evidence for a parasystolic mechanism in this record was overlooked by the investigators. The major NIB values for heart rates between 75 and 80 beats/min are 1, 4 and 6, whereas between 80 and 85 beats/min they are 1, 2 and 4. Between 85 and 90 beats/min the main values are 1, 2, 4 and 7, which may involve the two triplets 1, 2, 4 and 2, 4, 7. These NIB values are typical of a parasystolic mechanism (see Fig. 4).

Similar rhythms obeying the rules of pure parasystole were observed by Oreto et al. (29). Their first and fourth case reports show triplets of allowed NIB values of 1, 2, 4 and 1, 4, 6, respectively. They were able to derive phase response curves from the clinical data in both cases. We believe that the rules derived for pure parasystole are characteristic of quasiperiodic dynamics and may be an important diagnostic feature of parasystolic rhythms in general.

*Complex dynamics and chaos in modulated parasystole.* Previous experimental and theoretical studies have shown that oscillators stimulated with brief pulses can display complex rhythms including chaotic dynamics (9, 12, 13). Similar behavior was anticipated and found in the theoretical model of modulated parasystole. The NIB sequence obtained from the chaotic dynamics of Fig. 6 revealed some interesting features. The three most often encountered values in the sequence are 3, 6, and 9. A variant of concealed trigeminy with these numbers has been described by Levy and co-workers (20), where they

identify rhythms with NIB values of the form  $3n$ ,  $n$  any integer. However, in view of the significant fluctuations existing in parameters describing the human heartbeat (5), unambiguous identification of chaos in clinical records with frequent ectopy will be difficult. The origin of the fluctuations of the R-R interval in normal individuals is not understood. However, it is known that there are multiple controls regulating the heart rate (1). In the face of frequent ectopy and an ambient environment the complex control system will be expected to yield a fluctuating sinus rate. Such complex fluctuations may be "chaotic" (11). Disentangling the roles of the ambient environment, the multiple feedback control of heart rate and modulation in records with frequent ectopy is a challenge for future study.

This investigation has unearthed a number of intriguing theoretical questions about modulated parasystole. The fine structure of the histogram of Fig. 8 and the complex NIB zones of Fig. 4 require further study. These appear to contain an infinite amount of detail associated with the numerous entrainment zones present in the parameter space. It may be possible to predict the NIB values allowed even within the entrainment zones. Unravelling the sequences of bifurcations arising from the discontinuous forms of Eq. 1 will also be a formidable undertaking.

*Limitations of the analysis.* It is clear that the subtle dynamical variations of some arrhythmias (as in our first case, Fig. 7) are remarkably well accounted for by modulated parasystole. However, the applicability of modulated parasystole to the most frequently occurring complex arrhythmias is still not established. In particular our third case (Figs. 13–15) shows many features similar to previous case reports and presents a challenge for theoretical interpretation. In attempting to establish a PRC for this case (Fig. 2E) we found that there is a relatively fixed interval from sinus to ectopic beat (see APPENDIX). This is a common feature in clinical cases (25, 27, 28), and a classical interpretation of this finding is that the mechanism is reentry rather than parasystole. Fixed coupling restricts the location of sinus beats to small regions within the ectopic cycle where their effect can be determined. This underlies one of the major limitations of models of modulated parasystole. In many cases it is a somewhat arbitrary procedure to construct a PRC. It would clearly be of interest to establish computer algorithms to accomplish this task, but this has not yet been reported.

In attempting to simulate long rhythms, we have found that many of the subtle features that distinguish records are not easily accounted for in the models. Thus the computed transition matrices that we have used in this report may not show agreement with the data even though the NIB histograms do. Does this disprove the model? Or does it lead one to search for possible extensions that might give a better fit to the data? For example, based on excitability properties of cardiac tissue we expect refractory times of the ventricle and conduction times to and from the ectopic focus to show complex dependence on history (17, 33). However, it is difficult to understand the effects of such complex modifications on the dynamics of parasystole. As we have observed,

our attempts to establish models are confounded by the fluctuations in sinus rate. One way to overcome the problems associated with R-R fluctuation is to adapt a simple protocol based on our first case. This enables us to scan the whole range of possible rhythms in patients with frequent VPCs during controlled heart rate. In the case of parasystole (pure and modulated), the rhythm may be easily characterized by its behavior at different stimulation frequencies. Although intracardiac pacing is a delicate procedure, noninvasive testing that causes critical parameters to vary can be used in conjunction with dynamical analysis. For example, an exercise test in which a section of ECG of at least 1 or 2 min is obtained for each work level could provide an adequate scan of the dynamics as a function of heart rate. Similar tests are carried out routinely in the clinic, but little attention is paid to changes in the pattern of ectopy with heart rate. Earlier observations of change in ectopic frequency with heart rate often defy theoretical interpretation (36).

In nonlinear analysis, the changes in the dynamics of a system are characterized in terms of bifurcations as the value of parameters that control it are varied. In view of the findings in this study, we conclude that the human heart is one physiological system in which this type of analysis can yield valuable information about the nature of the mechanisms that govern its behavior in healthy and pathological conditions.

#### APPENDIX

The PRC gives the normalized perturbed ectopic cycle length ( $T/t_E$ ) as a function of the phase of the sinus beat ( $\phi$ ) and plays a crucial role in determining the dynamics of modulated parasystole. To construct a PRC from clinical data, it is necessary to assume that ectopic beats are generated by an ectopic pacemaker whose period in the absence of sinus beats is fixed. In the presence of sinus beats, the period is modulated. The amount of modulation depends on the phase(s) of the sinus beat(s) in the ectopic cycle. In many cases, it is also necessary to make assumptions about the location of concealed ectopic beats and the length of the intrinsic ectopic cycle. Here we present the major steps needed to establish the PRC and discuss some of the problems that arise in the context of our third case study.

The first step in determining the PRC is to evaluate the intrinsic ectopic cycle length ( $t_E$  in Fig. 2);  $t_E$  is obtained if successive ectopic beats are present, either as a result of medical intervention (25) or spontaneously (4, 35). This allows for the most precise determinations of the PRC by confirming the presence of an ectopic focus and provides a reference frame to assess the shortening or prolongation of  $t_E$ . In most clinical cases (15, 25, 27–29),  $t_E$  cannot be evaluated directly and may be estimated from the interectopic intervals containing a single sinus beat. If the intervening sinus beat shortens the ectopic cycle, the longest perturbed cycle ( $T$ ) observed can yield a first approximation for the value of  $t_E$ .

For the interectopic intervals containing a single sinus beat,  $T$  is given by the X-X interval, and  $\phi$  is obtained by dividing the length of the X-X interval by  $t_E$ . The plot of X-X vs. X-R intervals, therefore, gives valuable information about the PRC. If the X-R intervals cover a large portion of the (estimated) ectopic cycle length, the shape of the PRC will be evident from the plot (4, 25, 35). This is rarely the case. Points obtained in this way are often restricted to the last portion of the ectopic cycle where shortening occurs (Fig. 15 and Refs. 27–29). The

slope of the best line through these points gives the slope of the last portion of the PRC. In our report, although the R-X intervals do fluctuate by about  $\pm 40$  ms, X-X is approximately a linearly increasing function of the X-R interval with a slope close to 1 for X-R >800 ms.

As the X-R interval increases toward the value of the intrinsic ectopic period, the X-X interval should tend to the same value. This is often not the case (Fig. 15 and Ref. 29). In this situation, the last portion of the PRC would intersect the line  $T/t_E = 1$  at a value of  $\phi < 1$ . Sinus beats occurring at the latest phases would have no effect on the ectopic cycle. This is inconsistent with the resetting properties of most cardiac oscillators (2, 12, 16) and requires the presence of conduction delays. If there is anterograde conduction from the sinus pacemaker to the ectopic focus, the phase calculated as above for a single sinus beat within an interectopic interval is underestimated. This also occurs if there is retrograde conduction from the ectopic focus to the ventricles. The true phase of the sinus beat is given by  $(X-R + \text{anterograde conduction} + \text{retrograde conduction})/t_E$ . The X-X interval still represents the perturbed cycle length  $T$ . By including a conduction time, we obtain a correct PRC that intersects the line  $T/t_E = 1$  at  $\phi = 1$ .

In certain cases, a clear correspondence between the length of the X-R intervals and the NIB values exists. This may help to identify the crossover point between shortening and lengthening effects of sinus beats on the ectopic cycle. Oreto et al. (27) studied a case in which X-R intervals <950 ms were associated with NIB = 4, whereas X-R intervals >950 ms corresponded to NIB = 1. They assumed that the first sinus beat lengthened the ectopic cycle where NIB = 4 and shortened it where NIB = 1. This sets the crossover point at 950 ms. In our third case study, we do not observe any clear relation between X-R intervals and NIB values at a given heart rate. The model assumes that, within the range of X-R intervals observed, the first sinus beat of an interectopic interval always causes a shortening of the ectopic cycle.

The last step is to evaluate the lengthening effect of sinus beats occurring early in the ectopic cycle. Such a lengthening is always observed in experimental systems (2, 12, 16) and can be demonstrated by direct stimulation of the human heart (35). However, biphasic effects are only rarely observed in plots of X-X vs. X-R intervals from clinical data (4, 25). Most studies approximate the location of concealed ectopic discharges within the refractory period and calculate a PRC that fits the data (15, 27-29). We based our construction on qualitative arguments about the NIB values present in the clinical record. Consider the interectopic intervals containing three sinus beats. Because of conduction delays, the first sinus beat triggers an ectopic discharge that occurs  $\sim 700$  ms later. If the discharge falls outside the refractory period, NIB is equal to 1. If the discharge is concealed, the second sinus beat is allowed to modulate the ectopic cycle. Its phase can be computed based on the approximate location of the concealed ectopic beat. Because it occurs early, we assume that prolongation of the cycle takes place, so that the next ectopic discharge is now scheduled to occur between the third and fourth sinus beats. This explains the low number of NIB values equal to 2 in the record. The resulting modulated cycle length  $T$  can be calculated and a point placed on the PRC. The third sinus beat then occurs late in the ectopic cycle, triggering an ectopic beat and producing an interectopic interval containing three sinus beats. Although construction of the PRC based solely on clinical data is preferable, it is possible to analyse electrocardiographic records in light of numerical simulations that give good agreement with the length of intervals (X-R, R-X, X-X) observed. Experimental determination of the PRC then involves a reconstruction of the theoretical curve obtained in the simulation based on the data.

Regardless of the approximations involved in determining PRCs from clinical records, the models of modulated parasystole sometimes show striking agreement with complicated cardiac rhythms. In addition, the complete range of effects of sinus beats on an ectopic focus has been shown unambiguously in experimental systems and in certain clinical cases (2, 4, 12, 16, 25, 35). However, modulated parasystole may not always be the correct mechanism for complex rhythms with frequent ectopy, even when a PRC can be constructed. It is necessary to develop alternative hypotheses that can be tested quantitatively.

We thank B. Gavin for drafting the figures, T. Trabousee for technical assistance, and C. Pamplin and S. James for typing the manuscript.

This work has been partially supported by grants from the Natural Sciences and Engineering Research Council (NSERC) of Canada and the Canadian Heart Foundation to M. Courtemanche and L. Glass and by the Whitaker Health Sciences Fund National Heart, Lung, and Blood Institute Grant R01 HL-42172, and the G. Harold and Leila Y. Mathers Charitable Foundation to A. L. Goldberger.

M. Courtemanche was a recipient of a Postgraduate Scholarship from NSERC during 1987-1988 when this work was done.

Present address of M. Courtemanche: Dept. of Applied Mathematics, The University of Arizona, Tucson, AZ 85721.

Address for reprint requests: L. Glass, Dept. of Physiology, McGill University, 3655 Drummond St., Montreal, Quebec, H3G 1Y6 Canada.

Received 13 July 1988; accepted in final form 8 March 1989.

## REFERENCES

- AKSELROD, S., D. GORDON, F. A. UBEL, D. C. SHANNON, A. C. BARGER, AND R. J. COHEN. Power spectrum analysis of heart rate fluctuation: A quantitative probe of beat-to-beat cardiovascular control. *Science Wash. DC* 213: 220-222, 1981.
- ANTZELEVITCH, C., M. J. BERNSTEIN, H. N. FELDMAN, AND G. K. MOE. Parasystole, reentry, and tachycardia: a canine preparation of cardiac arrhythmias occurring across inexcitable segments of tissue. *Circulation* 68: 1101-1115, 1983.
- ANTZELEVITCH, C., AND G. K. MOE. Electrotonically mediated delayed conduction and reentry in relation to "slow responses" in mammalian ventricular tissue. *Circ. Res.* 49: 1129-1139, 1981.
- CASTELLANOS, A., R. M. LUCERI, F. MOLEIRO, D. S. KAYDEN, G. TROHMAN, L. ZAHMAN, AND R. J. MYERBURG. Annihilation, entrainment and modulation of ventricular parasystolic rhythms. *Am. J. Cardiol.* 54: 317-322, 1984.
- DEBOER, R. W., J. M. KAREMAKER, AND J. STRACKEE. Beat to beat variability of heart interval and blood pressure. *Automedica* 4: 217-222, 1983.
- DOWELL, A. R., C. E. BUCKLEY, R. COHEN, R. E. WHALEN, AND H. O. SIEKER. Cheyne-Stokes respiration. A review of clinical manifestations and critique of physiological mechanism. *Arch. Intern. Med.* 127: 712-726, 1971.
- FLEMING, G. B. Triple rhythm of the heart due to extrasystoles. *Q. J. Med.* 5: 318-326, 1912.
- GLASS, L., A. L. GOLDBERGER, AND J. BÉLAIR. Dynamics of parasystole. *Am. J. Physiol.* 251 (Heart Circ. Physiol. 20): H841-H847, 1986.
- GLASS, L., A. L. GOLDBERGER, M. COURTEMANCHE, AND A. SHRIER. Nonlinear dynamics, chaos and complex cardiac arrhythmias. *Proc. R. Soc. Lond. A Math. Phys. Sci.* 413: 9-16, 1987.
- GLASS, L., M. R. GUEVERA, J. BÉLAIR, AND A. SHRIER. Global bifurcations of a periodically forced biological oscillator. *Physiol. Rev.* 29: 1348-1357, 1984.
- GOLDBERGER, A. L., AND B. J. WEST. Chaos in physiology: health or disease? In: *Chaos in Biological Systems*, edited by H. Degn, A. V. Holden, and L. F. Olsen. New York: Plenum, 1987, p. 1-4.
- GUEVARA, M. R., L. GLASS, AND A. SHRIER. Phase-locking, period-doubling bifurcations and irregular dynamics in periodically stimulated cardiac cells. *Science Wash. DC* 214: 1350-1353, 1981.
- GUEVERA, M. R., A. SHRIER, AND L. GLASS. Phase-locked rhythms in periodically stimulated heart cell aggregates. *Am. J. Physiol.* 254

- (*Heart Circ. Physiol.* 23): H1-H10, 1988.
14. IKEDA, N., S. YOSHIZAWA, AND T. SATO. Difference equation model of ventricular parasystole as an interaction of pacemakers based on the phase response. *J. Theor. Biol.* 103: 439-465, 1983.
  15. JALIFE, J., C. ANTZELEVICH, AND G. K. MOE. The case for modulated parasystole. *Pace* 5: 911-926, 1982.
  16. JALIFE, J., AND G. K. MOE. Effect of electrotonic potentials on pacemaker activity in canine Purkinje fibers. *Circ. Res.* 39: 801-808, 1976.
  17. JANSE, M. J., A. B. M. VAN DER STEEN, R. T. VAN DAM, AND D. DURRER. Refractory period of the dog's ventricular myocardium following sudden changes in frequency. *Circ. Res.* 24: 257-262, 1969.
  18. LEE, M. H., M. N. LEVY, AND H. ZIESKE. Role of the compensatory pause in the production of concealed bigeminy. *Am. J. Cardiol.* 34: 697-703, 1974.
  19. LEVY, M. N., N. KERIN, AND I. EISENSTEIN. A subvariant of concealed bigeminy. *J. Electrocardiol.* 10: 225-232, 1977.
  20. LEVY, M. N., I. MORI, AND N. KERIN. Two variants of concealed trigeminy. *Am. Heart J.* 93: 183-188, 1977.
  21. MARRIOTT, H. J. L., AND M. H. CONOVER. *Advanced Concepts in Arrhythmias*. St. Louis, MO: Mosby, 1983.
  22. MENDEZ, C., C. C. GRUHZIT, AND G. K. MOE. Influence of cycle length upon refractory period of auricles, ventricles, and A-V node in the dog. *Am. J. Physiol.* 184: 287-295, 1956.
  23. MOE, G. K., J. JALIFE, W. J. MUELLER, AND B. MOE. A mathematical model of parasystole and its application to clinical arrhythmias. *Circulation* 56: 968-979, 1977.
  24. MOODY, G., AND R. MARK. Development and evaluation of a two-channel EKG analysis program. *Comput. Cardiol.* 9: 39-44, 1982.
  25. NAU, G. J., A. E. ALDARIZ, R. S. ACUNZO, M. S. HALPERN, J. M. DAVIDENKO, M. V. ELIZARI, AND M. B. ROSENBAUM. Modulation of parasystolic activity by nonparasystolic beats. *Circulation* 66: 462-469, 1982.
  26. NILSSON, G., S. BANDH, T. AHREN, K. CARLSON, T. JONASSON, AND I. RINGQVIST. Distribution patterns of ventricular premature complexes at different heart rates. *Am. J. Cardiol.* 59: 857-861, 1987.
  27. ORETO, G., F. LUZZA, G. SATULLO, S. COGLITORE, AND L. SCHAMROTH. Intermittent ventricular bigeminy as an expression of modulated parasystole. *Am. J. Cardiol.* 55: 1634-1637, 1985.
  28. ORETO, G., F. LUZZA, G. SATULLO, AND L. SCHAMROTH. Modulated ventricular parasystole as a mechanism for concealed bigeminy. *Am. J. Cardiol.* 58: 954-958, 1986.
  29. ORETO, G., G. SATULLO, F. LUZZA, A. DONATO, C. M. SACCA, F. ARRIGO, F. CONSOLO, AND L. SCHAMROTH. "Irregular" parasystole: the influence of sinus rhythm on a parasystolic focus. *Am. Heart J.* 115: 121-133, 1988.
  30. SCHAMROTH, L., AND H. J. L. MARRIOTT. Intermittent ventricular parasystole with observations on its relationship to extrasystolic bigeminy. *Am. J. Cardiol.* 7: 799-809, 1961.
  31. SCHAMROTH, L., D. H. MARTIN, AND M. PACHTER. The extrasystolic mechanism as the entrainment of an oscillator. *Am. Heart J.* 104: 1363-1368, 1988.
  32. SCHUSTER, H. G. *Deterministic Chaos*. Weinheim: VCH, 1988.
  33. SEED, W. A., M. I. M. NOBLE, P. OLDERSHAW, R. B. WANLESS, A. J. DRAKE-HOLLAND, D. REDWOOD, S. PUGH, AND C. MILLS. Relation of human cardiac action potential duration to the interval between beats: implications for the validity of rate corrected QT interval (QTc). *Br. Heart J.* 57: 32-37, 1987.
  34. SWENNE, C. A., P. A. DELANG, M. TEN HOOPEN, AND N. M. VAN HEMEL. Computer simulation of ventricular arrhythmias: ventricular bigeminy. *Comput. Cardiol.* 295-298, 1981.
  35. TENCZER, J., AND L. LITTMANN. Rate-dependent patterns of modulated ventricular parasystole. *Am. J. Cardiol.* 57: 576-581, 1986.
  36. WINKLE, R. A. The relationship between ventricular ectopic beat frequency and heart rate. *Circulation* 66: 439-446, 1982.
  37. WOLF, A., J. B. SWIFT, H. L. SWINNEY, AND J. A. VASTANO. Determining Lyapunov exponents from a time series. *Physica* 16D: 285-317, 1985.